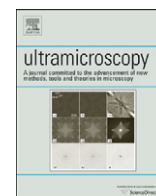




ELSEVIER

Contents lists available at [SciVerse ScienceDirect](http://www.sciencedirect.com)

Ultramicroscopy

journal homepage: www.elsevier.com/locate/ultramic

Influence of total beam current on HRTEM image resolution in differentially pumped ETEM with nitrogen gas

A.N. Bright^a, K. Yoshida^{b,c,*}, N. Tanaka^{c,d}^a FEI Company Japan Ltd., NSS-II Bldg 4F, 13-34 Kohnan 2-chome, Minato-ku, Tokyo 108-0075, Japan^b Institute of Advanced Research, Nagoya University, Chikusa-ku, Nagoya 464-8603, Japan^c Nanostructures Research Laboratory, The Japan Fine Ceramics Center, Nagoya 456-8587, Japan^d EcoTopia Science Institute, Nagoya University, Nagoya 464-8603, Japan

ARTICLE INFO

Article history:

Received 1 December 2011

Received in revised form

27 June 2012

Accepted 14 August 2012

Available online 24 August 2012

Keywords:

Environmental TEM

In-situ

Gas atmosphere

Differential pumping

HRTEM

Image resolution

Total beam current

Gas ionization

ABSTRACT

Environmental transmission electron microscopy (ETEM) enables the study of catalytic and other reaction processes as they occur with Angstrom-level resolution. The microscope used is a dedicated ETEM (Titan ETEM, FEI Company) with a differential pumping vacuum system and apertures, allowing aberration corrected high-resolution transmission electron microscopy (HRTEM) imaging to be performed with gas pressures up to 20 mbar in the sample area and with significant advantages over membrane-type E-cell holders. The effect on image resolution of varying the nitrogen gas pressure, electron beam current density and total beam current were measured using information limit (Young's fringes) on a standard cross grating sample and from silicon crystal lattice imaging. As expected, increasing gas pressure causes a decrease in HRTEM image resolution. However, the total electron beam current also causes big changes in the image resolution (lower beam current giving better resolution), whereas varying the beam current density has almost no effect on resolution, a result that has not been reported previously. This behavior is seen even with zero-loss filtered imaging, which we believe shows that the drop in resolution is caused by elastic scattering at gas ions created by the incident electron beam. Suitable conditions for acquiring high resolution images in a gas environment are discussed. Lattice images at nitrogen pressures up to 16 mbar are shown, with 0.12 nm information transfer at 4 mbar.

© 2012 Elsevier B.V. All rights reserved.

1. Introduction

The value of high-resolution transmission electron microscopy (HRTEM) images taken from samples while they are immersed in a gaseous environment is being increasingly recognized [1–5] and the recent availability of much improved dedicated environmental transmission electron microscopy (ETEM) instruments and holders is encouraging wider adoption. Many successful results have already been reported, particularly in the field of catalysis [1–13]. These researchers all used a differentially pumped ETEM system, which allows a pressure of about 20 mbar in the sample area while maintaining high vacuum in the region of the FEG [1,6,11,14], and without using gas-separation membranes. Several additional small apertures in the microscope column are used to separate regions at different gas pressure, which are pumped separately [5,6,11,14]. The alternative is an enclosed membrane

* Corresponding author at: Institute of Advanced Research, Nagoya University, Chikusa-ku, Nagoya 464-8603, Japan. Tel.: +81 52 789 3825; fax: +81 52 871 3500.

E-mail address: ky512@esi.nagoya-u.ac.jp (K. Yoshida).

holder to isolate the gas from the microscope vacuum. The design and function of a membrane E-cell holder is given in [15–17], the primary advantages being higher achievable gas pressure and lower system cost. Advantages of the differential pumping approach [1,14] include protection of the FEG, flexible use of normal holders, large field of view, usability at high temperature, high resolution imaging unobstructed by out of focus contrast from amorphous membranes, use in oxidizing environments without risk of membrane rupture, and improved reliability and repeatability of gas pressure measurement in the sample area. However, the achievable gas pressure is so far limited to around 20 mbar, and the gas path length (usually equal to the pole piece gap of the microscope) is normally 5.4 mm. E-cell holders with electron transparent membranes to contain the gas allow the use of higher gas pressures and the gas path length can be reduced [6,15–17].

In many ETEM applications the achievement of clear lattice contrast in the images greatly increases the value of the information obtained, and so one major goal of ETEM system development is to combine high gas pressure with high resolution imaging [2,3], which provides valuable information on crystal

structure, shape and orientation and is much improved by image resolution close to 0.1 nm [4–6,10]. Image quality and resolution in ETEM experiments can be limited by various factors, including sample drift (which tends to be much worse during heating experiments or after changing the gas flow rate) and image noise (if fast acquisition time or low dose imaging is required). However, the basic system performance under ideal conditions is determined by the system design. It is widely acknowledged that achievement of high resolution TEM imaging becomes more difficult as the gas pressure increases due to scattering of the electron beam by the gas molecules [1–3,5,14,17–20]. However, until the study of Jinschek and Helveg [20], the relationship between achievable HRTEM image resolution and gas pressure had never been reported in detail with only a few studies reporting experimental results or calculations [17,19], and the mechanism for resolution loss by gas scattering is still unclear. We have attempted to measure and understand the main factors contributing to the achievable image resolution on our ETEM system using a standard gas (nitrogen), and we here report the effect of varying the total electron beam current (at constant beam current density), which has not been reported previously.

2. Experimental procedure

The microscope used is a spherical aberration corrected ETEM (Titan ETEM 80-300, FEI Company) with a modified S-Twin objective lens (pole piece gap and gas path length of 5.4 mm), and SFEG gun. It was operated at 300 kV. The gas used was nominally 99.99999% pure nitrogen, the bottle located about 15 m from the system. The ETEM uses a differential pumping system to allow up to 20 mbar of gas in the sample area while maintaining about 8×10^{-9} mbar of vacuum in the FEG gun area.

Information limit (which is equal to the point resolution because of the image C_s corrector) was measured at 860kx magnification using a CCD camera (US1000, Gatan) on a Tridiem 863 energy filter (zero loss energy filtering had little effect on the results). The sample is a widely available cross grating sample consisting of a high density of AuPd metal crystallites on an amorphous carbon film (S106 cross grating, Agar). We used a 1 s exposure time, shifting the image by 1 nm halfway. Fast Fourier Transforms (FFTs or diffractograms) of the resulting images were taken using the Gatan Digital Micrograph software and the extent of Young's Fringes was measured. Information transfer was found or is known to depend on many factors, including the focus setting, sample type, e-beam damage, microscope alignment status, energy spread of the electron beam, chromatic aberration, beam intensity, image magnification, exposure time, and sample drift. These were controlled as much as possible to achieve useful comparison measurements.

Most users of HRTEM in materials science image crystalline material lattices, but there is no widely agreed way of evaluating the resolution or quality of such lattice images. Still, the extent of the FFT of a (well oriented) single crystal lattice sample does provide a useful guide to the image resolution, and the data is more repeatable than Young's fringes when gases are present in the chamber. Silicon lattice images were taken with similar settings to the information limit but without image shift.

Nitrogen gas pressure in the chamber was adjusted with needle-valves and measured using a gas-independent Barocell pressure gauge nearby. Software maintains the gas pressure at a constant level during the measurements. Current flowing through the fluorescent screen was used to measure the electron beam current (this reading is calibrated in the factory), and the beam current was adjusted by changing the condenser aperture size and first condenser lens (spot size).

'Total beam current' means the current measured on the fluorescent screen when (in the absence of gas or sample) all the electrons passing down the column hit it. The 2nd condenser lens (C2) was used to spread and converge the beam, resulting in a change in current density on the specimen, but almost no change in the total beam current. Increasing the C2 aperture size increases the illumination area on the fluorescent screen but results in no change in current density at the specimen (only the total current increases). Thus, total beam current (nA) and beam current density (A/cm^2) at the sample can be controlled independently, and their relative importance was investigated. The study of Jinschek [20] refers only to current density, which is the usual measure of beam intensity. The beam current density is equal to the total beam current divided by the illumination area on the sample, and this area was measured on the bottom mounted CCD camera (after this has been done once, the relative beam current densities can be calculated using the counts per pixel on the CCD).

3. Results and discussion

The reduction in TEM image resolution as the chamber gas pressure rises is known, but probably not well understood. Fig. 1 shows the effect of increasing nitrogen gas pressure on the TEM image resolution, using a constant total beam current of 1.3 nA as measured without gas or sample. Both information limit on AuPd/carbon (extent of Young's Fringes) and the extent of a diffractogram of a silicon $\langle 011 \rangle$ HRTEM lattice image are shown, as measures of resolution (a reference HRTEM image obtained from the AuPd/carbon sample is available as Fig. S1 in Supplementary material). The trends are similar, although the FFT extent for silicon is rather greater than the information limit (images are provided as Supplementary material, Fig. S2). The difference is notably larger at 16 mbar, perhaps because of the difficulty of accurately measuring the information limit at this pressure. Beam current density was adjusted to similar levels in each case so that CCD noise levels were about the same for all data points. Note that displayed screen current falls as gas pressure rises due to increased scattering or absorption [14], but the beam conditions were left unchanged. The information limit remains close to 0.10 nm up to 4 mbar, then drops to 0.13 nm at 8 mbar and about 0.23 nm at 16 mbar of nitrogen pressure, and silicon lattice information shows a corresponding drop, from 0.091 nm (the 244 reflexion) without gas to 0.15 nm with 16 mbar of nitrogen. So far this is as expected.

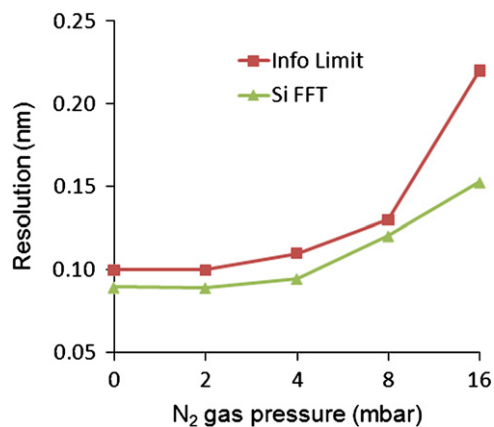


Fig. 1. Variation in TEM image resolution with increasing nitrogen gas pressure using a 1.3 nA total beam current. The upper line shows variation in information limit (Young's fringe extent) taken on a AuPd/carbon cross-grating sample. The lower line shows the extent of the diffractogram of a Si $\langle 011 \rangle$ single crystal lattice image.

The drop in transmitted beam current as the gas pressure rises (measured as fluorescent screen current), indicates strong interaction of the beam with the chamber gas. Current hitting the screen was found to drop by 4% at 1 mbar, 10% at 2 mbar, 21% at 4 mbar, 36% at 8 mbar and 58% at 16 mbar (all figures relative to the current without gas), and these percentages were found to be identical for starting total beam currents of 0.4 nA, 1.3 nA and 11 nA. This result is in good agreement with a previous study by Hansen [14]. The drop in resolution with increasing gas pressure is sometimes mentioned, for example by Hansen [5,14]. Contrast transfer calculations were performed by Yaguchi [17] using a membrane holder, who also achieved Si lattice imaging at 100 mbar with a 1 mm gas path length and states that angular spread and energy spread of the beam are the two main causes of resolution drop for HRTEM imaging through a gas cell. However the main study addressing gas pressure-dependent image resolution is that of Jinschek and Helveg [20], who performed extensive tests on an ETEM similar to the system used in this study at both 300 kV and 80 kV and compared nitrogen with hydrogen gas.

As the sample is placed approximately in the center of the gas region, elastic and inelastic scattering will occur both above and

below it in the chamber. Inelastic scattering, which is visible in the EELS spectrum of the gas with a strong edge onset at around 12 eV, can be filtered out using zero-loss filtered EFTEM. This was tested, and no significant improvement in the image resolution was seen by such energy filtering. The effectiveness of energy filtering for improving image resolution in gases at low magnification was reported by Sharma [18] but we did not find any such effect in these experiments. Such energy filtering should reduce or eliminate the image resolution loss caused by inelastic electron scattering, even where the scattering happens above the sample, and its ineffectiveness shows that another mechanism is operating. Hansen [14] suggests that a loss of coherence would be caused by the gas interaction but our results support elastic scattering as the dominant cause.

Fig. 2 shows Si $\langle 011 \rangle$ lattice images and AuPd/carbon information limit at constant 4 mbar nitrogen pressure as a function of the total electron beam current. The resolution can be dramatically improved just by reducing the total beam current, an effect which has never been reported and which needs to be explained in any model for the causes of resolution loss at high gas pressure. The Si data and information limit data correspond

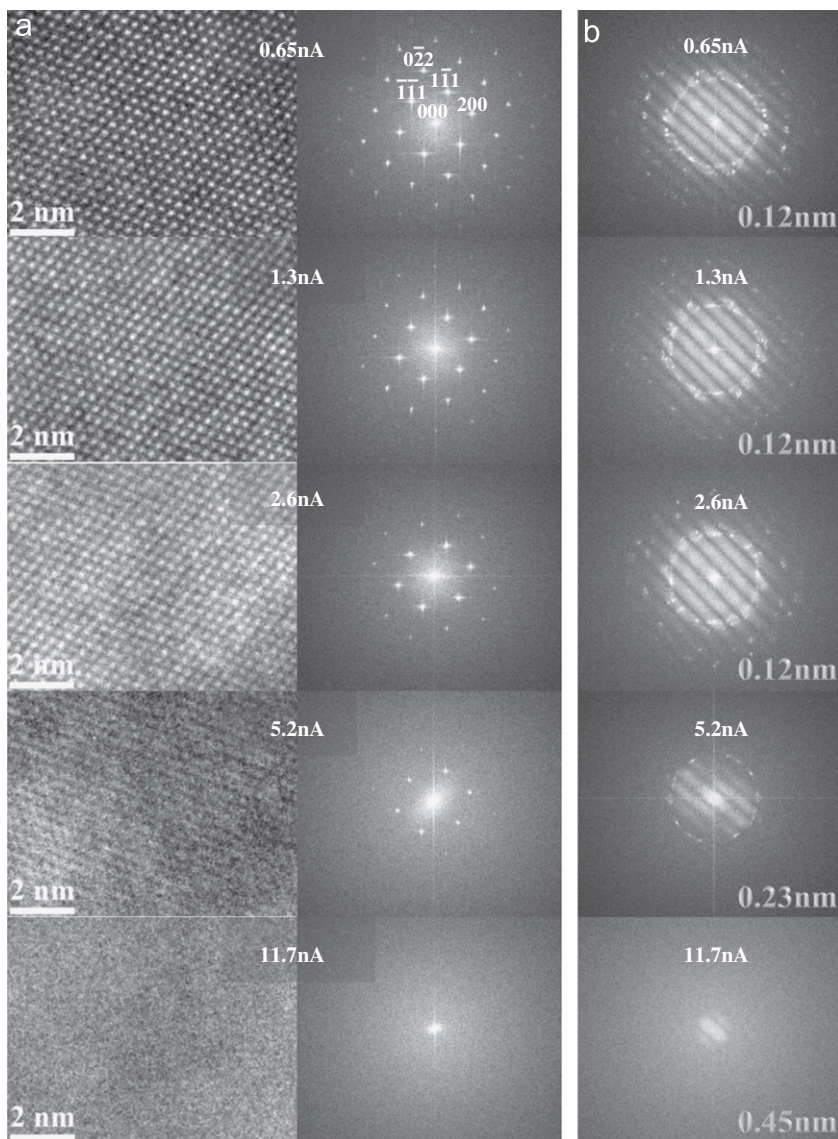


Fig. 2. HRTEM images taken with 4 mbar of nitrogen gas as a function of the total beam current (measured without gas). (a) Si $\langle 011 \rangle$ crystal lattice images with corresponding diffraction patterns, (b) Diffraction patterns of AuPd/carbon cross grating HRTEM images used for measurement of information limit (displayed bottom right).

well and are good evidence that the effect is not sample dependent, and is not caused by effects specific to measuring of Young's fringes on a grating membrane sample.

Importantly, no change in resolution was observed by changing the beam convergence, which changes the beam intensity hitting the specimen but not the total current. Fig. 3(a) shows the

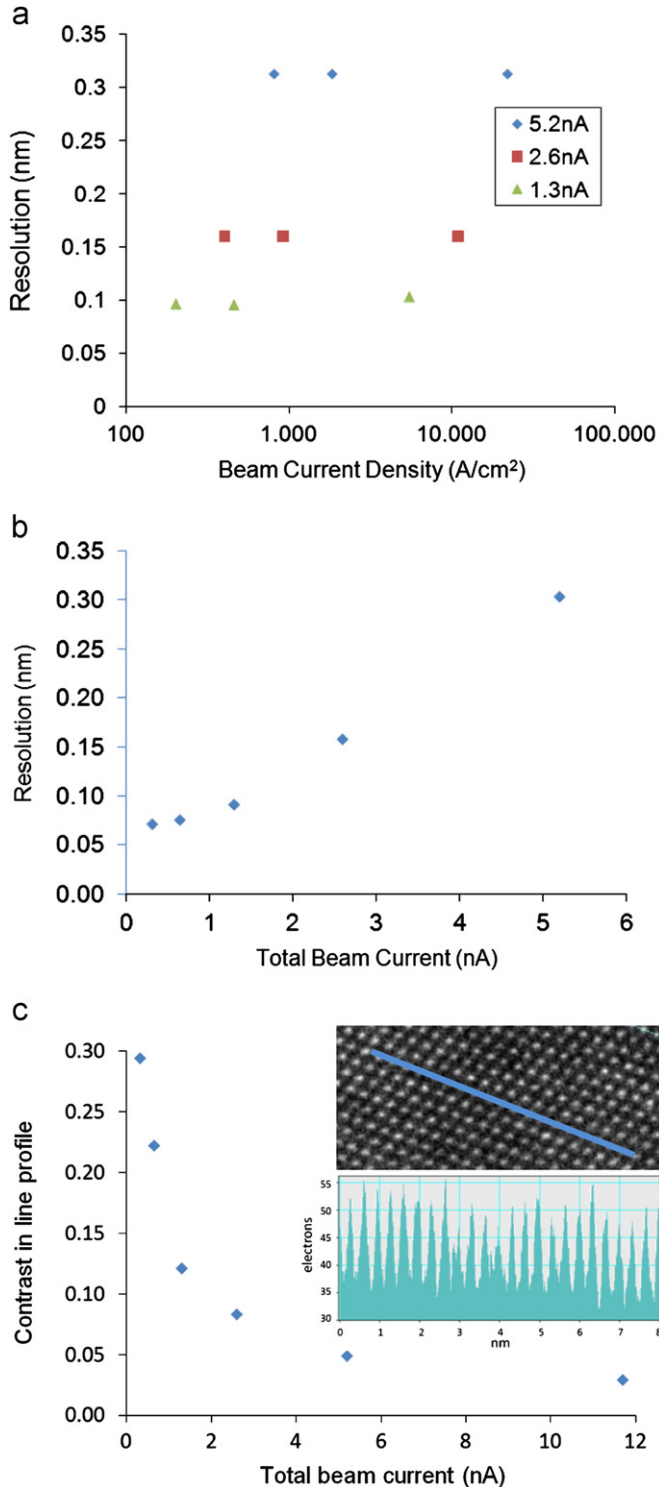


Fig. 3. Variation of HRTEM image resolution of $\langle 011 \rangle$ Silicon in 4 mbar of N_2 gas. (a) Effect of changing the beam current density at three different total beam currents, (b) Effect of varying the total beam current while maintaining a constant beam current density (5000 A/cm^2), (c) Variation in atomic row line profile contrast with increasing total beam current (example inset).

variation in resolution (extent of Si $\langle 110 \rangle$ HRTEM lattice image FFT) as a function of varying beam current density for three different total beam currents (1.3 nA, 2.6 nA and 5.2 nA), all taken through a 10 eV zero loss energy filtering slit. The resolution stays constant even when beam current density is increased by a factor of 27, whereas the variation in resolution with total beam current at a constant beam current density, Fig. 3(b), is very clear (the current density was 5000 A/cm^2). Only the total beam current significantly affects resolution.

Signal to noise in the lattice images decreases with increasing beam current. The variation in lattice contrast with increasing beam current is shown in Fig. 3(c), measured using line profiles of a row of Si atomic columns. Contrast figures shown are $(I_{\max} - I_{\min}) / (I_{\max} + I_{\min})$. This is a more direct way of measuring the drop in lattice information with beam current (or gas pressure) increase, but the result is comparable. Contrast measurements are rather sensitive to the sample quality, orientation, thickness and damage, but the trend is repeatable. The profiles at each current are shown in Supplementary material (Fig. S3).

Thus, in general to achieve high resolution imaging in this nitrogen gas environment the beam current should be kept low and beam convergence maximized, maintaining just enough current to keep a sufficient signal to noise ratio in the images while fully covering the CCD with the beam. Increasing magnification can help if it allows greater beam convergence without the beam edges becoming visible on the CCD, and screen current of 0.1 nA or below was found to still give good lattice information with a 1 s exposure time, even at 20 mbar of nitrogen, which is the gas pressure limit of the microscope. Fig. 4 shows Si $\langle 011 \rangle$

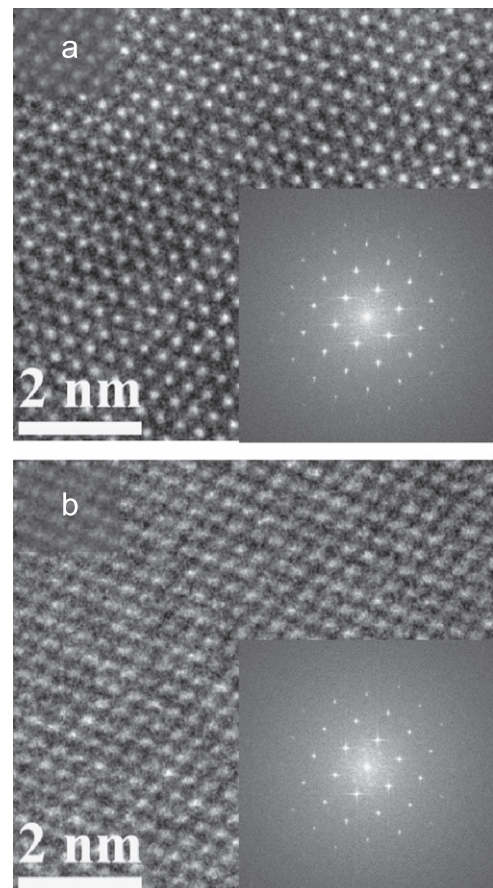


Fig. 4. HRTEM of Si $\langle 011 \rangle$ and diffractograms showing the achievable lattice image quality using low beam current with (a) 8 mbar of N_2 gas, 0.65 nA total beam current, (b) 16 mbar of N_2 gas, 0.17 nA total beam current.

lattice images taken with 8 mbar and 16 mbar of nitrogen gas, where the beam current has been roughly optimized.

The overall beam current is the key parameter (rather than current density on the sample or CCD). This is illustrated by the observed lattice resolution drop when you increase the condenser lens aperture size while looking at an HRTEM image, where none of the extra electrons should normally reach the CCD (and the measured CCD count rate was unchanged). This means the image resolution is reduced by electrons which do not reach the CCD. This is illustrated in [Supplementary material, Fig. S4](#). We believe the most likely explanation is ionization of gas molecules in the beam to form a kind of plasma in the sample chamber. The ions move to the imaging region and cause elastic scattering of the electron beam, leading to pronounced tails on the central spot of the diffraction pattern at high gas pressures (see Jinschek [20]). In the case of neutral gas molecules, elastic scattering would be mostly at the gas nuclei (which scatter less, due to shielding, and to higher angles). Two other key results reported by Jinschek [20] need to be explained. First, the resolution drop at increased gas pressure is much sharper with 80 kV electrons than 300 kV electrons—this is probably because the ionization cross section is much higher at 80 kV so a greater number of molecules become ionized, and also that 80 kV electrons, traveling slower, are scattered more strongly by these ions. Second, the drop in resolution is much less pronounced in hydrogen gas than in nitrogen. H^+ and N^+ ions with the same charge should cause a similar level of elastic scattering, so we suggest that fewer ions are created by the electron beam in the case of hydrogen, or that the hydrogen ions have a shorter lifetime or leave the beam area more quickly due to their small mass. A full understanding will require effective modeling of the behavior of the gas under the electron beam and of the electron beam passing through the ionized gas, which is beyond the scope of this paper.

4. Conclusions

High resolution TEM lattice imaging can be performed in the presence of gases in a differentially pumped ETEM system. Image resolution decreases with increasing gas pressure, but the effect can be reduced substantially by using a low electron beam current. The effects of total beam current and beam current density on image resolution were studied, and the resolution was found to be independent of beam current density, but strongly dependent on the total beam current, a result that has not been published previously. This dependence, seen in both zero-loss filtered and unfiltered HRTEM images, suggests that elastic scattering of electrons at gas ions created by the electron beam is the main cause. The previous results of Jinschek [20] showed a much stronger resolution drop using 80 kV electrons than 300 kV, and a much stronger drop using nitrogen gas than hydrogen. These results can be explained by a higher probability of gas ionization and higher scattering of electrons at 80 kV, and by a higher ionization probability of nitrogen molecules or a longer ion lifetime relative to hydrogen.

A good model of the effect of beam current will be necessary to fully understand the mechanisms behind the drop in TEM image resolution as the gas pressure increases in an ETEM system. Clear understanding of these results will help ETEM users to achieve better high resolution imaging results in gas environments. Using the ETEM we achieved HRTEM imaging with clear $Si <011>$ lattice contrast using gas pressures up to 16 mbar (and 0.12 nm information limit at 4 mbar) by using suitable beam current conditions. In general, HRTEM image resolution in gases can be improved by reducing gas pressure, reducing total electron beam current or designing the environmental cell so as to reduce the

gas path length of the electron beam [1,5,12,14,17]. In the case of ETEM work low beam current is also important for reducing the influence of the electron beam on the sample structure and gas reactions [1,4,5,19]. More sensitive cameras [2,7] to allow high quality imaging at low dose (as well as high speed) will thus be important in the development of future ETEM systems.

Acknowledgments

This work was partly supported by Grant-in-Aid for Young Scientific Researcher (B) 24710110 from the Japan Society for the Promotion of Science (JSPS). The ETEM facility is partly supported by grants from the Chubu Economic Federation and Aichi Prefecture. We thank Dr. Y. Sasaki of JFCC for ETEM usage. We also thank Dr. J. R. Jinschek of FEI Company for valuable discussions about the differential pumping system and the influence of gases on HRTEM imaging.

Appendix A. Supporting information

Supplementary data associated with this article can be found in the online version at <http://dx.doi.org/10.1016/j.ultramic.2012.08.007>.

References

- [1] E.D. Boyes, P.L. Gai, Environmental high resolution electron microscopy and applications to chemical science, *Ultramicroscopy* 67 (1997) 219–232.
- [2] P.L. Gai, Developments in in situ environmental cell high-resolution electron microscopy and applications to catalysis, *Topics in Catalysis* 21–4 (2002) 161–173.
- [3] H. Topsoe, Developments in operant studies and in situ characterization of heterogeneous catalysts, *Journal of Catalysis* 216 (2003) 155–164.
- [4] P.A. Crozier, R. Wang, R. Sharma, In situ TEM studies of dynamic changes in cerium-based oxides nanoparticles during redox process, *Ultramicroscopy* 108 (2008) 1432–1440.
- [5] P.L. Hansen, S. Helveg, A.K. Datye, Atomic-scale imaging of supported metal nanocluster catalysts in the working state, *Advances in Catalysis* 50 (2006) 77–95.
- [6] R. Sharma, An environmental transmission electron microscope for in situ synthesis and characterization of nanomaterials, *Journal of Materials Research* 20–7 (2005) 1695–1707.
- [7] P.C.K. Vesborg, Ib Chorkendorff, Ida Knudsen, Olivier Balmes, Jesper Nerlov, Alfons M. Molenbroek, Bjerne S. Clausen, Stig Helveg, Transient behavior of Cu/ZnO-based methanol synthesis catalysts, *Journal of Catalysis* 262 (2009) 65–72.
- [8] H. Yoshida, Tetsuya Uchiyama, Hideo Kohno, Seiji Takeda, Environmental transmission electron microscopy observations of the growth of carbon nanotubes under nanotube–nanotube and nanotube–substrate interactions, *Applied Surface Science* 254 (2008) 7586–7590.
- [9] H. Yoshida, Seiji Takeda, Tetsuya Uchiyama, Hideo Kohno, Yoshikazu Homma, Atomic-scale in-situ observation of carbon nanotube growth from solid state iron carbide nanoparticles, *Nano Letters* 8–7 (2008) 2082–2086.
- [10] S. Helveg, P.L. Hansen, Atomic-scale studies of metallic nanocluster catalysts by in situ high-resolution transmission electron microscopy, *Catalysis Today* 111 (2006) 68–73.
- [11] Q. Jeangros, A. Faes, J.B. Wagner, T.W. Hansen, U. Aschauer, J. Van herle, A. Hessler-Wyser, R.E. Dunin-Borkowski, In situ redox cycle of a nickel-YSZ fuel cell anode in an environmental transmission electron microscope, *Acta Materialia* 58 (2010) 4578–4589.
- [12] R. Sharma, Design and applications of environmental cell transmission electron microscope for in situ observations of gas–solid reactions, *Microscopy and Microanalysis* 7 (2001) 494–506.
- [13] H. Yoshida, Y. Kuwauchi, J.R. Jinschek, K. Sun, S. Tanaka, M. Kohyama, S. Shimada, M. Haruta, S. Takeda, Visualizing gas molecules interacting with supported nanoparticulate catalysts at reaction conditions, *Science* 335 (2012) 317–319.
- [14] T.W. Hansen, J.B. Wagner, R.E. Dunin-Borkowski, Aberration corrected and monochromated environmental transmission electron microscopy: challenges and prospects for materials science, *Materials Science and Technology* 26–11 (2010) 1338–1344.
- [15] J.F. Creemer, S. Helveg, G.H. Hovelings, S. Ullmann, A.M. Molenbroek, P.M. Sarro, H.W. Zandbergen, Atomic-scale electron microscopy at ambient pressure, *Ultramicroscopy* 108 (2008) 993–998.
- [16] T. Kawasaki, K. Ueda, M. Ichihashi, T. Tanji, Improvement of windowed type environmental-cell transmission electron microscope for in situ

- observation of gas–solid interactions, *Review of Scientific Instruments* 80 (2009) 11370-1–113701-5.
- [17] T. Yaguchi, M. Suzuki, A. Watabe, Y. Nagakubo, K. Ueda, T. Kamino, Development of a high temperature-atmospheric pressure environmental cell for high-resolution TEM, *Journal of Electron Microscopy* 60–3 (2011) 217–225.
- [18] R. Sharma, K. Weiss, Development of a TEM to study in situ structural and chemical changes at an atomic level during gas–solid interactions at elevated temperatures, *Microscopy Research and Technique* 42 (1998) 270–280.
- [19] H. Yoshida, S. Takeda, Image formation in a transmission electron microscope equipped with an environmental cell: single-walled carbon nanotubes in source gas, *Physical Review B* 72 (2005) 195428-1–195428-7.
- [20] J.R. Jinschek, S. Helveg, Image resolution and sensitivity in an environmental transmission electron microscope, *Micron* 43 (2012) 1156–1168.